The Astronomical Journal, 142:92 (9pp), 2011 September doi:10.1088/0004-6256/142/3/92

THE SOLAR NEIGHBORHOOD. XXVII. DISCOVERY OF NEW PROPER MOTION STARS WITH $\mu \geqslant 0\farcs18$ yr^{-1} IN THE SOUTHERN SKY WITH $16.5 < R_{59F} \leqslant 18.0$

Mark R. Boyd[1], Todd J. Henry[1], Wei-Chun Jao[1], John P. Subasavage[2], and Nigel C. Hambly[3]
[1] Georgia State University Department of Physics and Astronomy, Atlanta, GA 30302-4106, USA;
boyd@chara.gsu.edu, thenry@chara.gsu.edu, jao@chara.gsu.edu
[2] Cerro Tololo Inter-American Observatory, La Serena, Chile; jsubasavage@ctio.noao.edu
[3] Scottish Universities Physics Alliance, Institute for Astronomy, University of Edinburgh, Royal Observatory, Blackford Hill, Edinburgh EH9 3HJ, Scotland, UK; nch@roe.ac.uk
Received 2011 June 3; accepted 2011 July 19; published 2011 August 16

ABSTRACT

Here we present 1584 new southern proper motion systems with $\mu \geqslant 0\farcs18$ yr^{-1} and $16.5 > R_{59F} \geqslant 18.0$. This search complements the six previous SuperCOSMOS-RECONS (SCR) proper motion searches of the southern sky for stars within the same proper motion range, but with $R_{59F} \leqslant 16.5$. As in previous papers, we present distance estimates for these systems and find that three systems are estimated to be within 25 pc, including one, SCR 1546-5534, possibly within the RECONS 10 pc horizon at 6.7 pc, making it the second nearest discovery of the searches. We find 97 white dwarf candidates with distance estimates between 10 and 120 pc, as well as 557 cool subdwarf candidates. The subdwarfs found in this paper make up nearly half of the subdwarf systems reported from our SCR searches and are significantly redder than those discovered thus far. The SCR searches have now found 155 red dwarfs estimated to be within 25 pc, including 10 within 10 pc. In addition, 143 white dwarf candidates and 1155 cool subdwarf candidates have been discovered. The 1584 systems reported here augment the sample of 4724 systems previously discovered in our SCR searches and imply that additional systems fainter than $R_{59F} = 18.0$ are yet to be discovered.

Key words: astrometry – solar neighborhood – stars: distances – stars: low-mass – stars: statistics – surveys

Online-only material: machine-readable and VO tables

1. INTRODUCTION

The Research Consortium On Nearby Stars (RECONS)[4] has completed surveying the southern sky for proper motion objects with R_{59F} (hereafter R) brighter than 16.5 mag using a specialized trawl of the individual plate detections comprising the SuperCOSMOS Sky Survey (SSS) database, with new discoveries dubbed SCR (SuperCOSMOS-RECONS). These results have been detailed in six papers in the The Solar Neighborhood (TSN) series: Hambly et al. (2004), Henry et al. (2004), Subasavage et al. (2005a, 2005b), Finch et al. (2007), and Boyd et al. (2011) (TSN VIII, X, XII, XV, XVIII, and XXV, respectively). This seventh proper motion search paper complements the previous six by searching the entire southern sky for objects with the same lower proper motion cutoff of $\mu \geqslant 0\farcs18$ yr^{-1} as in previous papers, while examining objects fainter than the previous R cutoff. In this paper we stretch our search from $R = 16.5$ to 18.0 to reveal stars intrinsically fainter than found in previous searches, as well as stars similar to previous discoveries but at larger distances. In previous searches, it was found that several stars, including SCR 1845-6357AB, the 23rd nearest system (as of 2011 January 1), had R between 16.0 and 16.5, very near the search cutoff. It is natural, then, to assume that there may be more very nearby systems just beyond this cutoff that have heretofore gone unnoticed.

Despite far outnumbering their brighter counterparts, intrinsically faint nearby stars are underrepresented in the census of nearby stars, as evidenced by the discovery of many nearby red dwarfs (Henry et al. 2006) and white dwarfs (WDs; Subasavage et al. 2009). In particular, of the 256 systems with accurate parallaxes placing them within 10 pc, 174 (68%) have primaries of spectral type M. This search has been designed specifically to detect such faint objects. This effort is the latest in a long line of searches that revealed faint nearby stars, such as the classic sky surveys by Giclas et al. (1971, 1978) and Luyten (1979, 1980b). Many more surveys have since been done utilizing modern technology but fundamentally similar techniques and are discussed in TSN XXV and references therein.

In this paper, we present photometric distance estimates for the red dwarf systems found during this search. Using the relations of Hambly et al. (2004), we estimate three red dwarfs to be within 25 pc, including one estimated to be at 6.7 pc. Using reduced proper motion (RPM) diagrams, we also identify 97 WD candidates, 7 of which may be within 25 pc (see Section 5.2). Particularly noteworthy for this survey, we report 557 new cool subdwarf candidates, nearly doubling the total identified during the SCR searches. The 1584 systems and 1608 objects reported in this paper bring the total number of SCR systems to 6308, consisting of 6650 objects.[5] Identifying comprehensive samples of proper motion objects now will prepare us for large-scale astrometric surveys such as LSST and *Gaia*, as well as provide precursor investigation opportunities. Ultimately, these new groups of intrinsically faint objects will help develop accurate models of the Galaxy as a whole.

2. SEARCH CRITERIA AND METHODOLOGY

This search has been performed with methods similar to those discussed in previous TSN papers. In brief, we make use of SuperCOSMOS scans of at least three Schmidt survey

[4] www.recons.org

[5] Note that systems are only counted if all components are new discoveries. Multiples consisting of two SCR objects are counted once, while multiples with at least one known component are not counted toward the number of new systems.

photographic plates taken of each field. The photographic plates scanned into the SuperCOSMOS database are 6° × 6° with a 0.°5 overlap on each side, giving ∼25° square of unique sky coverage per field (in order to streamline computations of astrometric and photometric data, the overlap regions were not used). For this search, we have examined 893 of 894 fields, with one omitted because of an insufficient epoch spread and a location too near the Galactic plane. Thus, this search encompasses the entire southern sky save for one region 25° square.

For this search, we require the *R* magnitude to be between 16.5 and 18.0 mag, with the brighter limit corresponding to the faint limit of previous searches, and the fainter limit being chosen to reveal late M dwarfs out to 10 pc. At 25 pc, we estimate that red dwarfs with spectral types earlier than M7.5V will have apparent *R* magnitudes greater than 18.0, with this search specifically targeting M5.5V to M7.5V.

We have used similar plate ellipticity requirements as TSN XXV: any object with two or more ellipticities greater than 0.35 is excluded. This requirement was shown in TSN XXV to eliminate significant amounts of false detections while removing no real proper motion objects in a trial sample of ∼200 stars. The ellipticity checks, along with the three-plate detection requirement preserves high-quality candidates that went undetected on a single plate. SCR 1845-6357AB (Hambly et al. 2004), for example, was undetected on the *B* plate. Finally, we exclude objects with R_{ESO} and *R* magnitudes differing by more than 1.0 mag in an effort to eliminate variable giant stars. We find 7626 initial candidates on these plates.

This list of candidates was then checked using Aladin by blinking the B_J, *R*, and I_{IVN} (hereafter *BRI*) plates with a 5′ radius to confirm that the objects are truly moving. Two Micron All Sky Survey (2MASS) JHK_s (hereafter *JHK*) magnitudes, coordinates, and observation epochs were extracted for confirmed proper motion objects that were then checked against SIMBAD and other proper motion surveys (e.g., NLTT—Luyten 1980a, LEHPM—Pokorny et al. 2003, SIPS—Deacon et al. 2005, UPM—Finch et al. 2010) using VizieR to determine which objects are new SCR discoveries. In both Vizier and SIMBAD, a region 90″ in radius was used to match candidate objects to published objects, in accordance with the findings of Bakos et al. (2002), who found that coordinates of stars in the Luyten half-second (LHS) catalog were usually accurate to within ∼90″ (see their Figure 2). In the blinking process, several common proper motion (CPM) candidates were noted that were not extracted in the initial trawl, but were found by eye (see Section 5.5).

3. COMPARISON TO PREVIOUS SEARCHES

Here we compare the discovery statistics of this effort to previous SCR searches. We continue to use the terminology used in TSN XXV to describe the various proper motion bins called MOTION, SLOWMO, and MINIMO, which contain systems with $\mu \geqslant 1.''00$ yr^{-1}, $1.''00$ yr^{-1} > $\mu \geqslant 0.''50$ yr^{-1}, and $0.''50$ yr^{-1} > $\mu \geqslant 0.''18$ yr^{-1}, respectively. The two lower cutoffs were chosen to match those of the LHS and Luyten Two Tenths (LTT) catalogs, respectively. The results are summarized in Table 1, where the first number in each column is from previous searches while the second is from this effort. We note that significant amounts of garbage (i.e., false detections) were found in this search. These candidates, as in previous searches in high proper motion regimes, are primarily detections with erroneously high proper motion data. Matching high proper motion objects across epochs is more prone to mismatches than matching slow-moving or non-moving objects, particularly at faint magnitudes, hence the amount of garbage at higher proper motions is significantly larger.

Table 1
Discovery Statistics for the Entire SCR Sample to Date[a]

Category	MOTION[b]	SLOWMO[c]	MINIMO[d]	Total[e]
New discoveries	9 + 0	141 + 9	4574 + 1575	6308
Known	171 + 11	1159 + 133	17244 + 4090	22808
Duplicates	15 + 1	91 + 3	1640 + 356	2106
Garbage	1989 + 700	344 + 17	5335 + 28	8413
Total hits	2184 + 712	1735 + 162	28793 + 6049	39635

Notes.
[a] A few objects were also reported in searches done concurrently by Deacon et al. (2005), Deacon & Hambly (2007), Lépine (2005), and Lépine (2008).
[b] MOTION sample includes $\mu \geqslant 1.''00$ yr^{-1}.
[c] SLOWMO sample includes $1.''00$ yr^{-1} > $\mu \geqslant 0.''50$ yr^{-1}.
[d] MINIMO sample includes $0.''50$ yr^{-1} > $\mu \geqslant 0.''18$ yr^{-1}.
[e] All SCR searches to date.

We also update the hit rates—the sums of new, known, and duplicate objects divided by the total starting sample of all candidate objects—for each proper motion bin. Known objects are defined as those found to be previously discovered by other groups as outlined in Section 2, whereas duplicates are objects for which more than one hit was returned from the SuperCOSMOS database. Garbage objects are those that are returned from the search but were found to be erroneous point source matches that were not verified to be proper motion objects. The new hit rates for the SCR sample are 7.1%, 81.0%, and 84.6% for the MOTION, SLOWMO, and MINIMO samples, respectively. The MOTION hit rate is slightly lower than the most recent update in TSN XXV due to the substantial amounts of garbage found in this search, while hit rates for the other two samples are somewhat higher, due to search criteria excluding excessive garbage in those proper motion bins.

In the NLTT catalog, there are 4356 objects that meet the criteria of this search. Of these, we recover 2782, or 63%, which is somewhat lower than the 71% recovered during the search in TSN XXV. Our cumulative total of 6308 systems for our entire southern hemisphere search represents an increase of 24.6% over the 25616 entries in the southern NLTT catalog.

4. DATA

In Table 2, we list the first five of the 1608 newly discovered objects. All 1608 objects are listed in the online version of the journal. We provide SCR names, J2000.0 coordinates, SuperCOSMOS proper motions and position angles, *BRIJHK* magnitudes, the $(R - J)$ color, and a distance estimate. We report a total of 1584 systems, which is less than the number of objects because (1) some systems have more than one SCR object and (2) systems including both a known and SCR object are not included in the number of systems. We list red dwarfs within 25 pc, WDs, and cool subdwarfs in Tables 3, 4, and 5, respectively. The WDs and subdwarfs have been selected according to the criteria outlined in Section 5.2. Multiple systems are listen in Table 6 and discussed in Section 5.5.

TSN XVIII and XXV, as well as Finch et al. (2010), compare SuperCOSMOS data to data from various catalogs such as *Hipparcos*, *Tycho*, PPMX, and PPMXL. The results indicate that the SCR proper motions are consistent to other sources to ∼$0.''02$ yr^{-1} in both R.A. and decl. The details of those comparisons can be found in TSN XVIII and XXV.

Table 2
New SCR Objects with $16.5 < R_{59F} \leqslant 18.0$

Name	R.A. (J2000)	Decl. (J2000)	μ ($''$ yr^{-1})	θ (°)	B_J	R_{59F}	I_{IVN}	J	H	K_s	$(R_{59F} - J)$	Est Dist (pc)	Notes
SCR 0001-8110	00 01 06.59	−81 10 38.0	0.232	103.5	18.60	16.80	14.61	13.40	12.88	12.63	3.40	118.2	
SCR 0001-1037	00 01 39.89	−10 37 51.9	0.185	171.9	19.62	17.63	15.78	14.13	13.52	13.28	3.50	136.9	
SCR 0001-1744	00 01 43.45	−17 44 49.9	0.187	093.4	19.08	17.49	15.44	13.63	13.04	12.81	3.86	104.5	
SCR 0001-4236	00 01 46.24	−42 36 23.2	0.181	108.4	20.00	17.88	17.10	16.51	15.62	16.25	1.37	[1148.7]	a
SCR 0005-0159	00 05 25.63	−01 59 58.7	0.182	194.0	18.94	16.89	14.77	13.44	12.88	12.60	3.45	104.6	

Note. [a] Cool subdwarf candidate—unreliable distance.

(This table is available in its entirety in machine-readable and Virtual Observatory (VO) forms in the online journal. A portion is shown here for guidance regarding its form and content.)

Table 3
New 25 pc Red Dwarf Candidates

Name	R.A. (J2000)	Decl. (J2000)	μ ($''$ yr^{-1})	θ (°)	B_J	R_{59F}	I_{IVN}	J	H	K_s	$(R_{59F} - J)$	Est Dist (pc)	Notes
SCR 1144-4302	11 44 24.88	−43 02 53.5	0.311	293.6	19.60	17.50	14.39	12.17	11.56	11.20	5.33	24.7	
SCR 1546-5534	15 46 41.84	−55 34 47.0	0.433	226.8	18.99	17.22	14.03	10.21	9.55	9.11	7.01	6.7	a
SCR 1609-3431	16 09 46.19	−34 31 06.9	0.249	198.5	18.48	16.61	13.99	11.58	10.99	10.67	5.03	22.5	

Note. [a] Distance suspect. See Section 5.7.

The distance estimates in Tables 2, 3, 5, and 6 have been derived using the suite of 11 plate relations in Hambly et al. (2004), which utilizes the six photometry values—*BRI* plate magnitudes from SuperCOSMOS and *JHK* from 2MASS—associated with each object. That paper and TSN XXV describe errors associated with the relations in more detail. The plate photometry errors are ∼0.3 mag, while 2MASS data errors are typically less than ∼0.03 mag. The relations fail for blue stars, as well as WDs and most subdwarfs. For this reason, we list such objects' distances in brackets in the Tables 2, 3, 5, and 6. WDs have more accurate distances listed in the notes of Tables 2, 4, and 6.

5. ANALYSIS

In this search we have found a few red dwarfs estimated to be within 25 pc, as well as many WD and cool subdwarf candidates. The numbers in these categories, however, are significantly different from previous papers. We find only three red dwarfs within 25 pc, listed in Table 3. We estimate the nearest, SCR 1546-5534, to be at 6.7 pc. If this estimate holds true, it will become the second nearest object found by the SCR searches, after SCR 1845-6357AB at 3.5 pc (Henry et al. 2006). We find a total of 97 WDs using two RPM diagrams (see Section 5.2), tripling the total number of candidates from previous SCR searches, during which we found 46. Seven of the candidates from this search are estimated to be within 25 pc. Of particular note, we find 557 new cool subdwarf candidates, many of which are redder than those previously found. This total nearly doubles the 598 found in all previous SCR searches and comprises over one-third of the sample in this paper. The remaining objects are likely to be early- to mid-type M dwarfs beyond 25 pc.

5.1. Color–Magnitude Diagram

Figure 1 shows the color–magnitude diagram for all SCR discoveries to date. Discoveries from the previous six searches are marked with small circles, while those presented here are marked with large circles. This search reveals sources that are redder than previous searches. Of note is the point at $(R - J)$ $= 7.01$, which is SCR 1546-5534, the nearest and reddest system discovered by this search. The bluest objects are all WD candidates, with the bluest being SCR 0221-0143, with $(R - J) = 0.12$.

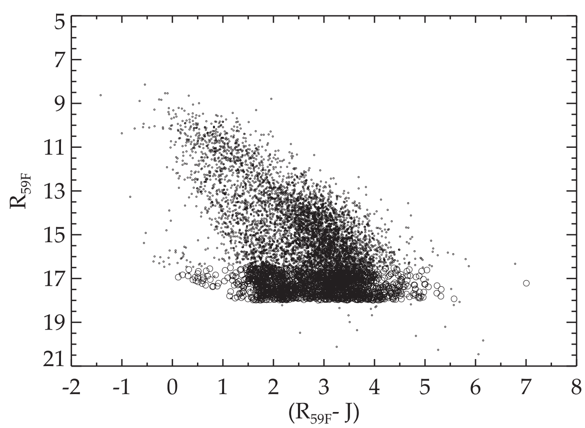

Figure 1. Color-apparent magnitude plot for all SCR discoveries. Discoveries from this paper are marked with open circles, while those from previous papers are marked with small circles. Scattered points below $R_{59F} = 16.5$ are CPM companions noticed by eye.

While not as easily discerned as in previous papers, the WD and subdwarf regions are visible, with the WDs extending to the left of $(R - J) = 1.0$ and the subdwarfs found between $(R - J)=$ 1.0 and $(R - J) \sim 2.5$. Further discussion of those systems can be found in the next three sections.

5.2. Reduced Proper Motion Diagram

Figures 2 and 3 show RPM diagrams for SCR objects found during the present survey. The RPM diagram is a powerful tool for estimating the luminosity class of a star. It is similar in nature to the H-R diagram except that the distance is replaced by the star's proper motion, relying on the inverse statistical relationship between proper motion, μ, and distance. While obviously not foolproof—for example, WDs may mimic subdwarfs, and vice versa in the RPM diagram—the diagram

Table 4
New SCR White Dwarf Candidates

Name	R.A. (J2000)	Decl. (J2000)	μ ($'' \text{ yr}^{-1}$)	θ ($^\circ$)	B_J	R_{59F}	I_{IVN}	J	H	K_s	Est. Dist.[a] (pc)	Notes
Candidates Selected Using ($R_{59F} - J$) RPM Diagram												
SCR 0058-6905	00 58 43.53	−69 05 41.7	0.331	120.4	19.78	17.20	16.70	15.94	15.49	15.65	12.1	
SCR 0128-7401	01 28 52.26	−74 01 53.6	0.209	089.8	19.30	16.97	16.25	15.87	15.29	15.16	12.8	
SCR 0153-0730B	01 53 12.29	−07 30 30.6	0.465	150.0	19.73	17.89	17.20	16.32	15.70	15.56	28.3	b
SCR 0205-7941	02 05 24.81	−79 41 03.7	0.194	098.0	17.21	17.06	16.91	16.65	16.31	15.74	65.5	
SCR 0221-0143	02 21 14.88	−01 43 40.4	0.323	219.1	17.49	16.94	16.80	16.82	16.40	16.38	46.5	
SCR 0243-6034	02 43 00.34	−60 34 14.5	0.245	178.0	17.80	16.77	16.32	16.27	15.89	15.37	30.4	
SCR 0345-8652	03 45 53.24	−86 52 31.1	0.183	012.7	17.28	17.01	16.93	16.39	16.32	15.27	59.2	
SCR 0616-4122	06 16 22.05	−41 22 31.4	0.181	348.3	17.42	16.97	16.70	16.47	16.11	16.04	50.8	
SCR 0626-3752	06 26 00.05	−37 52 18.2	0.293	138.6	18.47	17.59	17.22	16.44	16.30	16.33	49.8	
SCR 0637-7410	06 37 24.25	−74 10 59.3	0.233	025.4	17.56	17.10	16.87	16.50	16.11	15.71	53.6	
SCR 0712-0428	07 12 06.17	−04 28 16.0	0.218	341.2	18.19	17.21	16.92	16.30	16.12	15.53	38.8	
SCR 0816-4641	08 16 30.13	−46 41 13.2	0.441	060.7	18.27	16.88	16.18	15.68	15.59	14.91	24.7	
SCR 0825-5107	08 25 33.14	−51 07 30.9	0.332	301.7	17.73	16.86	16.66	15.68	15.34	15.25	35.5	
SCR 0855-0833	08 55 34.71	−08 33 45.0	0.467	188.9	18.79	17.31	16.77	16.08	15.84	15.28	28.0	
SCR 0913-3910B	09 13 12.40	−39 10 19.0	0.232	248.2	17.61	17.11	16.68	16.09	17.48	15.40	52.6	b
SCR 0913-6851	09 13 32.27	−68 51 36.5	0.344	320.2	17.91	17.35	16.93	16.55	15.93	16.07	56.1	
SCR 1016-3616	10 16 22.15	−36 16 44.4	0.202	327.6	17.42	16.95	16.73	16.50	16.34	15.37	49.3	
SCR 1126-0931	11 26 34.26	−09 31 15.2	0.283	241.4	20.27	17.99	17.18	16.34	15.59	15.43	21.4	
SCR 1129-7823	11 29 24.40	−78 23 57.7	0.211	264.7	17.48	17.35	17.20	16.46	16.14	15.83	76.0	
SCR 1156-3655	11 56 04.30	−36 55 48.0	0.207	269.6	18.45	17.67	17.30	16.34	16.95	15.60	55.2	
SCR 1203-3621	12 03 34.26	−36 21 05.1	0.259	300.2	17.28	16.89	16.59	16.19	15.98	15.74	50.9	
SCR 1204-3514	12 04 48.89	−35 14 27.9	0.242	261.9	17.69	17.31	16.88	16.65	15.85	16.76	62.2	
SCR 1216-3758	12 16 16.94	−37 58 48.0	0.275	191.6	19.37	17.90	17.41	16.66	16.50	15.65	37.1	
SCR 1224-0018	12 24 22.91	−00 18 18.6	0.208	271.9	17.60	16.88	16.42	16.57	16.35	15.51	40.0	
SCR 1241-0733	12 41 40.12	−07 33 06.0	0.182	280.5	17.00	16.83	16.72	16.63	17.66	16.28	58.6	
SCR 1243-3926	12 43 38.77	−39 26 46.1	0.185	209.8	17.58	17.15	16.83	16.64	16.34	15.66	56.1	
SCR 1351-3912	13 51 09.73	−39 12 51.4	0.282	139.6	17.67	16.65	16.28	15.98	15.66	15.84	29.0	
SCR 1416-6531	14 16 22.46	−65 31 26.8	0.337	258.8	17.00	16.67	16.67	16.16	16.09	15.57	48.1	
SCR 1452-0011	14 52 24.95	−00 11 34.9	0.288	218.1	19.48	17.38	16.32	16.58	15.74	15.47	18.3	
SCR 1600-1654	16 00 41.16	−16 54 30.2	0.812	284.0	19.30	17.84	17.22	16.56	16.27	16.57	36.4	
SCR 1601-3832	16 01 37.02	−38 32 09.2	0.326	124.5	18.01	17.08	16.80	15.89	15.86	15.59	37.5	
SCR 1751-7749B	17 51 39.55	−77 49 02.6	0.341	188.0	17.43	16.93	16.70	16.32	15.70	15.37	48.0	b
SCR 2008-8051	20 08 14.23	−80 51 08.4	0.214	180.8	18.16	17.79	17.57	16.66	17.07	15.82	78.8	
SCR 2045-1411	20 45 43.03	−14 11 31.7	0.831	170.6	20.24	17.39	15.99	15.11	14.57	14.57	10.7	
SCR 2101-3509	21 01 26.68	−35 09 33.4	0.184	250.9	17.10	16.59	16.21	16.26	16.09	15.50	40.6	
SCR 2105-3247	21 05 24.18	−32 47 32.7	0.193	257.2	16.93	16.55	16.29	15.81	15.53	15.67	44.1	
SCR 2108-0312	21 08 54.88	−03 12 03.1	0.192	187.6	17.82	16.84	16.29	15.98	15.93	15.96	32.4	
SCR 2110-1158	21 10 11.80	−11 58 33.2	0.262	106.2	17.68	16.63	16.06	15.58	15.16	15.23	27.9	
SCR 2140-5124	21 40 44.77	−51 24 14.5	0.190	188.3	17.80	17.23	16.97	16.64	17.54	16.96	52.7	
SCR 2153-0214	21 53 42.11	−02 14 26.6	0.277	092.3	17.58	17.10	16.86	16.64	16.04	17.06	53.1	
SCR 2225-2007	22 25 48.57	−20 07 31.1	0.277	114.8	17.81	17.05	16.56	16.30	16.12	15.88	41.8	
SCR 2331-4907	23 31 55.99	−49 07 42.2	0.217	153.7	19.86	17.66	17.11	16.29	15.41	15.78	19.6	
Candidates Selected Using ($B - R_{59F}$) RPM Diagram[c]												
SCR 0019-1113	00 19 42.07	−11 13 58.0	0.246	112.4	18.05	17.68	17.39	...	...	...	74.6	
SCR 0055-1504	00 55 46.25	−15 04 51.0	0.278	101.2	17.42	17.26	17.35	...	...	...	71.6	
SCR 0117-1659	01 17 52.23	−16 59 26.0	0.198	248.2	18.67	17.75	17.33	...	...	...	51.8	
SCR 0120-7851	01 20 15.88	−78 51 43.0	0.180	166.1	16.83	16.86	16.82	...	...	...	68.7	
SCR 0148-1824	01 48 31.64	−18 24 55.0	0.193	119.0	18.46	17.79	17.60	...	...	...	63.2	
SCR 0211-1434	02 11 51.89	−14 34 48.0	0.197	096.4	17.47	17.32	17.37	...	...	...	74.2	
SCR 0220-6936	02 20 48.49	−69 36 32.0	0.267	079.6	18.71	17.84	17.41	...	...	...	56.2	
SCR 0226-6200	02 26 55.97	−62 00 38.0	0.183	054.6	17.39	17.30	17.13	...	...	...	77.0	
SCR 0256-0700	02 56 41.59	−07 00 33.0	0.423	118.1	19.06	17.79	17.39	...	...	...	40.6	
SCR 0321-2930	03 21 59.47	−29 30 33.0	0.274	082.4	18.83	17.89	17.80	...	...	...	54.2	
SCR 0331-4118	03 31 57.25	−41 18 06.0	0.213	208.8	18.50	17.57	17.24	...	...	...	47.2	
SCR 0353-6514	03 53 33.20	−65 14 18.0	0.187	027.3	18.08	17.65	17.67	...	...	...	70.9	
SCR 0401-7643	04 01 31.44	−76 43 52.0	0.231	025.5	18.71	17.88	17.48	...	...	...	58.3	
SCR 0411-1353	04 11 51.39	−13 53 55.0	0.201	179.9	18.42	17.99	18.00	...	...	...	82.6	
SCR 0506-5510	05 06 40.16	−55 10 52.0	0.182	035.0	17.42	17.16	16.95	...	...	...	63.7	
SCR 0632-6503	06 32 24.12	−65 03 59.0	0.236	014.5	18.38	17.88	17.79	...	...	...	74.5	
SCR 0737-6347	07 37 30.65	−63 47 34.0	0.287	310.1	18.27	17.67	17.55	...	...	...	62.7	
SCR 0805-1702	08 05 03.23	−17 02 18.0	0.420	295.2	17.59	17.48	17.67	...	...	...	82.0	
SCR 0809-1234	08 09 36.45	−12 34 03.0	0.402	150.2	19.22	17.96	17.42	...	...	...	44.8	
SCR 0815-7344	08 15 35.63	−73 44 31.0	0.186	349.0	18.86	17.95	17.34	...	...	...	56.5	

Table 4
(Continued)

Name	R.A. (J2000)	Decl. (J2000)	μ (″ yr^{-1})	θ (°)	B_J	R_{59F}	I_{IVN}	J	H	K_s	Est. Dist.[a] (pc)	Notes
SCR 0836-3318	08 36 38.24	−33 18 05.0	0.272	131.2	18.21	17.65	17.50	...	...	...	63.9	
SCR 0853-6733	08 53 47.44	−67 33 32.0	0.231	336.6	18.60	17.91	17.69	...	...	...	66.0	
SCR 0859-1700	08 59 16.81	−17 00 55.0	0.180	311.4	17.18	17.15	17.21	...	...	...	75.0	
SCR 0859-6925	08 59 24.18	−69 25 06.0	0.295	291.2	18.52	17.83	17.40	...	...	...	63.1	
SCR 0914-1534	09 14 04.90	−15 34 06.0	0.233	166.2	18.71	17.77	17.40	...	...	...	51.2	
SCR 0930-3944	09 30 50.87	−39 44 04.0	0.182	145.2	17.60	17.55	17.71	...	...	...	88.5	
SCR 1020-0436	10 20 55.99	−04 36 24.0	0.202	164.9	18.42	17.97	17.68	...	...	...	80.8	
SCR 1037-0818	10 37 37.77	−08 18 22.0	0.187	250.0	18.28	17.75	17.57	...	...	...	68.5	
SCR 1103-7109	11 03 20.12	−71 09 58.0	0.195	271.2	18.36	17.83	17.53	...	...	...	71.4	
SCR 1104-5002	11 04 42.01	−50 02 58.0	0.277	270.8	18.94	18.00	17.60	...	...	...	56.8	
SCR 1128-0537	11 28 04.46	−05 37 17.0	0.328	142.2	18.35	17.50	17.32	...	...	...	48.4	
SCR 1139-0846	11 39 24.46	−08 46 39.0	0.182	298.4	17.00	16.90	16.92	...	...	...	63.2	
SCR 1206-0722	12 06 05.68	−07 22 28.0	0.240	211.1	18.86	17.77	17.27	...	...	...	46.4	
SCR 1227-4558	12 27 33.08	−45 58 00.0	0.186	290.0	18.94	17.97	17.50	...	...	...	54.8	
SCR 1314-0438	13 14 24.47	−04 38 12.0	0.201	239.4	18.05	17.40	17.10	...	...	...	53.3	
SCR 1316-3633	13 16 05.10	−36 33 07.0	0.207	143.8	16.92	16.95	17.10	...	...	...	71.3	
SCR 1331-7743	13 31 44.96	−77 43 02.0	0.337	247.6	18.33	17.98	17.83	...	...	...	86.6	
SCR 1339-0937	13 39 39.29	−09 37 07.0	0.295	246.3	18.92	17.79	17.50	...	...	...	45.3	
SCR 1340-1517	13 40 01.12	−15 17 33.0	0.450	272.4	18.69	17.70	17.32	...	...	...	47.7	
SCR 1347-4848	13 47 43.65	−48 48 47.0	0.373	218.3	18.67	17.94	17.51	...	...	...	64.9	
SCR 1402-0902	14 02 12.89	−09 02 45.0	0.229	259.6	18.08	17.70	17.58	...	...	...	74.8	
SCR 1403-1514	14 03 42.83	−15 14 13.0	0.392	205.8	18.81	17.86	17.45	...	...	...	53.1	
SCR 1418-1157	14 18 44.12	−11 57 14.0	0.181	263.5	18.11	17.71	17.84	...	...	...	74.0	
SCR 1556-0805	15 56 47.31	−08 05 59.0	0.421	117.9	18.80	17.84	18.06	...	...	...	52.3	
SCR 1802-4907	18 02 58.31	−49 07 33.0	0.284	184.0	17.05	16.72	16.64	...	...	...	49.3	
SCR 1848-4619	18 48 09.12	−46 19 56.0	0.208	196.3	17.71	17.81	17.80	...	...	...	112.4	
SCR 1904-5851	19 04 34.30	−58 51 16.0	0.185	161.7	17.93	17.56	17.39	...	...	...	70.7	
SCR 1945-3338	19 45 21.46	−33 38 47.0	0.213	234.2	18.64	17.99	17.88	...	...	...	70.3	
SCR 2049-4237	20 49 55.23	−42 37 35.0	0.226	126.1	18.98	17.87	17.40	...	...	...	47.4	
SCR 2052-4212	20 52 21.29	−42 12 58.0	0.311	139.5	19.02	17.93	17.32	...	...	...	49.2	
SCR 2108-1127	21 08 37.58	−11 27 58.0	0.228	119.3	17.08	16.99	16.99	...	...	...	66.9	
SCR 2115-0741A	21 15 07.44	−07 41 33.0	0.212	187.0	17.09	17.08	16.91	...	...	...	73.7	b
SCR 2240-7829	22 40 44.71	−78 29 45.0	0.226	110.0	17.99	17.72	17.54	...	...	...	81.8	
SCR 2319-0255	23 19 35.92	−02 55 24.0	0.216	249.2	18.37	17.55	17.33	...	...	...	50.8	
SCR 2334-5111	23 34 49.32	−51 11 51.0	0.188	095.3	17.87	17.32	17.08	...	...	...	55.5	

Notes.
[a] Estimate given using relation of Oppenheimer et al. (2001).
[b] CPM system—see Table 6.
[c] Candidates lack 2MASS data. Coordinates not J2000.0.

Table 5
New SCR Cool Subdwarf Candidates

Name	R.A. (J2000)	Decl. (J2000)	μ (″ yr^{-1})	θ (°)	B_J	R_{59F}	I_{IVN}	J	H	K_s	$(R_{59F} - J)$	Est. Dist. (pc)	Notes
SCR 0001-4236	00 01 46.24	−42 36 23.2	0.181	108.4	19.96	17.88	17.10	16.51	15.62	16.25	1.37	[1148.7]	
SCR 0008-0028	00 08 26.27	−00 28 50.3	0.192	177.8	18.65	16.89	16.09	15.30	14.79	14.54	1.59	[507.9]	
SCR 0016-0021	00 16 31.20	−00 21 11.3	0.191	091.6	18.79	17.08	16.19	15.14	14.51	14.30	1.94	[432.2]	
SCR 0017-5825	00 17 45.97	−58 25 56.0	0.195	167.3	19.89	17.79	16.65	15.43	15.11	14.88	2.36	[500.1]	
SCR 0017-6821	00 17 57.95	−68 21 53.3	0.193	114.7	19.98	17.97	16.73	15.70	15.08	14.79	2.27	[468.1]	

(This table is available in its entirety in machine-readable and Virtual Observatory (VO) forms in the online journal. A portion is shown here for guidance regarding its form and content.)

allows for the rough classification of systems. The equation used here to determine the pseudo-absolute magnitude $H_{R_{59F}}$ plotted on the vertical axis of Figure 2 is

$$H_{R_{59F}} = R_{59F} + 5 + 5 \log \mu .$$

The dashed line used to separate WD and subdwarf candidates in Figure 2 is the same as in RPM diagrams in previous papers. The solid lines, as in TSN 25, denote the cool subdwarf region. Cool subdwarfs are defined as having $(R - J) > 1.0$ and are within four magnitudes of the WD line. These definitions of both the WD and subdwarf regions are, of course, arbitrary, but have proven to be reliable in selecting high-quality candidates. We find a total of 42 WD candidates and 557 cool subdwarf candidates in this plot.

New to our SCR searches, we have included a second RPM diagram in addition to the $(R - J)$ version. To reveal WDs too

Table 6
Common Proper Motion Systems

Primary	μ ($'' \text{yr}^{-1}$)	θ (°)	Distance (pc)	Companion(s)	μ ($'' \text{yr}^{-1}$)	θ (°)	Distance (pc)	Sep. ($''$)	P.A. (°)	Notes
				Probable Common Proper Motion Systems						
L 044-086	0.318	188.7	46.7	SCR 1751-7749B	0.341	188.0	[674.2]	135.3	0.4	WD candidate at 48.0 pc[ab]
LEHPM2-2868	0.184	121.6	85.4	SCR 0253-1738B	0.184	119.4	140.3	102.1	179.9	[a]
LEHPM2-5029	0.183	227.0	372.5	SCR 1312-3103B	0.196	219.8	131.9	650.7	289.4	
SCR 0115-1226A	0.192	109.4	123.9	SCR 0114-1227B	0.196	116.2	163.9	464.8	186.7	
SCR 0153-0731A	0.452	140.7	[217.8]	SCR 0153-0730B	0.465	150.0	[800.1]	55.5	343.2	WD candidate at 28.3 pc[ac]
SCR 0219-7102A	0.275	041.0	137.0	SCR 0219-7102B	0.264	043.8	205.5	34.7	275.3	
SCR 0307-4654A	0.190	060.9	191.5	LEHPM1-3098	0.194	059.1	146.9	1180.3	54.7	
SCR 0335-4019A	0.188	046.7	80.6	SCR 0336-4028B	0.184	051.7	159.9	1036.6	122.0	
SCR 0913-3910A	0.233	250.0	61.4	SCR 0913-3910B	0.232	248.2	[660.5]	12.8	174.2	WD candidate at 52.6 pc[ab]
SCR 1018-0130A	0.204	229.4	[599.3]	SCR 1017-0143B	0.214	236.7	[430.0]	1039.1	232.3	[c]
SCR 1352-0205A	0.226	266.6	234.5	SCR 1352-0157B	0.224	266.4	121.5	548.9	61.2	
SCR 2211-4825A	0.183	116.0	161.3	SCR 2210-4835B	0.181	116.9	140.0	1143.0	212.5	
				Possible Common Proper Motion Systems						
SCR 0203-0727A	0.248	169.2	[677.8]	SCR 0203-0727B	...	...	...	15.3	339.3	[bc]
SCR 0424-2427A	0.181	094.5	126.2	LEHPM2-5525	0.180	128.6	112.6	183.1	29.4	
SCR 0443-5732A	...	...	...	SCR 0443-5731B	0.259	063.8	[697.9]	32.6	14.7	[c]
SCR 0728-2211A	...	...	...	SCR 0728-2211B	0.263	181.1	99.5	20.7	13.8	[b]
SCR 0729-8402A	...	...	...	SCR 0729-8402B	0.270	350.6	[489.6]	456.6	94.8	[bc]
SCR 1051-0008A	0.269	180.0	56.5	SCR 1051-0009B	...	...	...	...	...	[bd]
SCR 1351-0115A	0.218	278.0	[234.6]	SCR 1351-0118B	0.188	267.4	231.8	221.0	224.2	[c]
				SCR 1352-0106C	0.205	276.9	247.7	879.6	38.2	[c]
SCR 1418-4725A	0.185	191.8	69.2	SCR 1418-4725B	...	...	...	...	...	[bd]
SCR 1602-0225A	0.189	220.7	104.0	SCR 1602-0225B	0.184	205.1	76.4	32.9	215.4	
SCR 1612-4829A	...	...	...	SCR 1612-4830B	0.194	234.0	71.9	161.6	212.9	[b]
SCR 2115-0741A	0.212	187.0	...	SCR 2115-0744B	0.235	160.5	140.0	...	...	WD candidate at 73.7 pc[abd]
SCR 2236-6030A	...	...	...	SCR 2236-6029B	0.260	125.4	[320.4]	80.3	20.9	[bc]

Notes.
[a] WD candidate with unreliable distance estimate [in brackets]. More accurate estimate in notes if available. See Table 4.
[b] Companion detected by eye during blinking process.
[c] Cool subdwarf candidate with unreliable distance estimate [in brackets]. See Table 5.

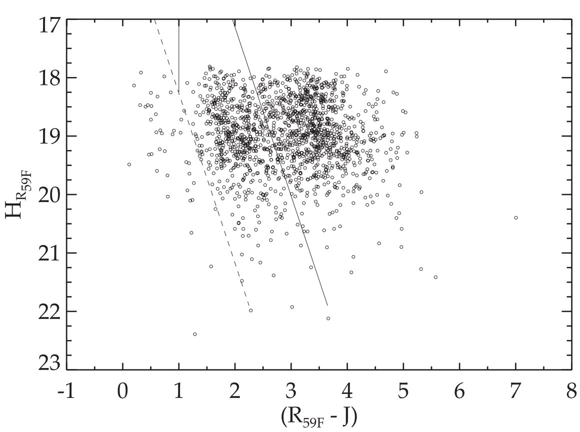

Figure 2. $(R - J)$ reduced proper motion diagram. The dashed line separates white dwarfs from subdwarfs, while the solid lines, along with the dashed line, outline the cool subdwarf region.

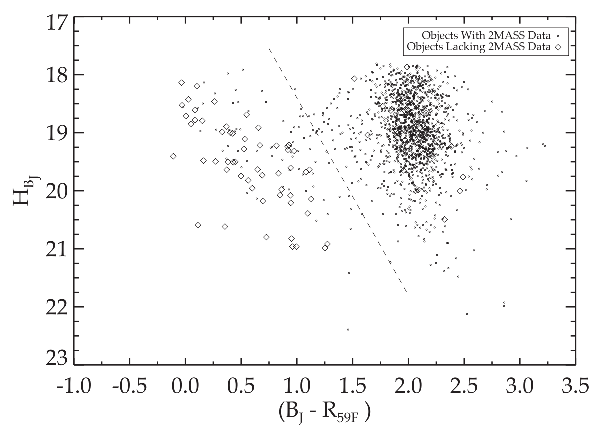

Figure 3. $(B - R)$ reduced proper motion diagram. The dashed line separates white dwarfs from subdwarfs and red dwarfs. Objects lacking 2MASS data are marked with diamonds. All such objects below the dashed line have been selected as WD candidates.

faint to be in 2MASS, we use the $(B - R)$ color because many WDs will not show up in 2MASS given our search limits of $16.5 < R \leqslant 18.0$ and the typical $(R - J) < 1.0$ color of WDs. In order to calculate H_B we use the equation above, substituting B for R. We use the same WD–subdwarf cutoff line as Oppenheimer et al. (2001) to identify an additional 55 WD candidates. We do not select any more cool subdwarf candidates because subdwarfs and main-sequence stars are indistinguishable in this RPM diagram. Further discussion of WDs and subdwarfs can be found in Sections 5.3 and 5.4.

5.3. New White Dwarf Candidates

We find a total of 97 new WD candidates using the two RPM diagrams, presented in Table 4 and divided into two categories based on the RPM diagram from which they were selected.

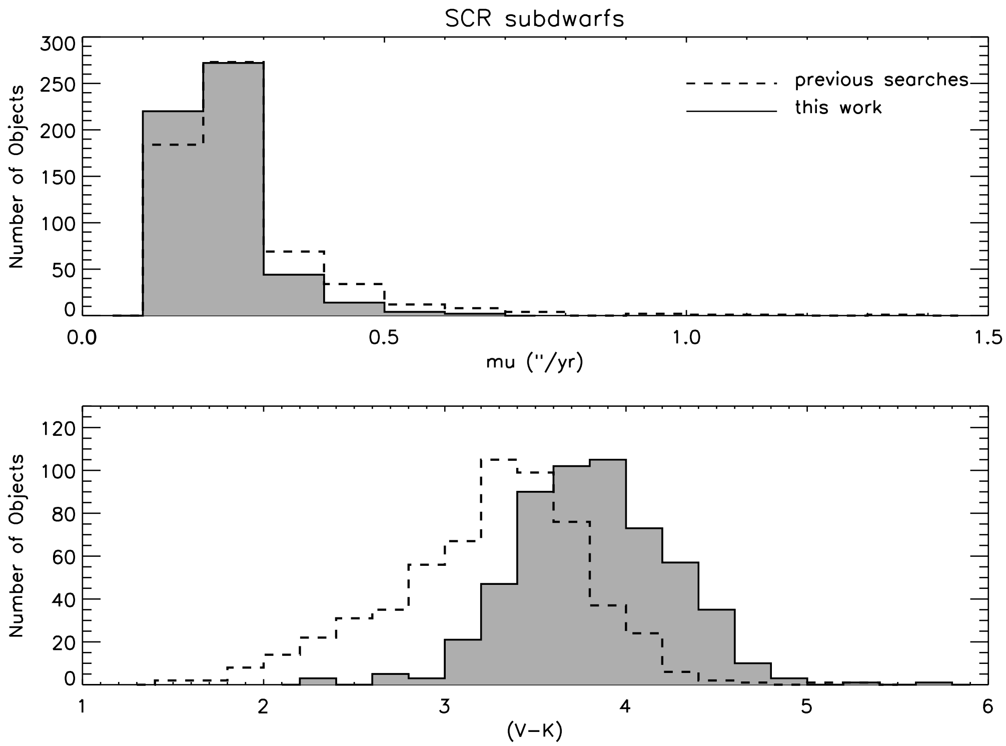

Figure 4. Histograms of SCR subdwarf candidates reported in this paper (filled) and previous TSN papers (outlined). The top plot shows quantity vs. proper motion bin, while the bottom shows quantity vs. color. There are notably fewer high proper motion discoveries in this paper, but those subdwarf candidates discovered tend to be redder than previous discoveries.

We present the same data as Table 2 except in lieu of the inaccurate distance estimates generated assuming the objects are red dwarfs, we give distances based on the single color linear relation of Oppenheimer et al. (2001), assuming the objects are WDs. We find seven WDs estimated to be within 25 pc, all from the $(R - J)$ RPM diagram. Of these, five have either optical or IR colors that are redder than typical WDs. Two, SCR 0058-6905 and SCR 0816-4641, do appear to be good nearby WD candidates. Three of the seven 25 pc candidates presented lie within the 13 pc horizon within which Holberg et al. (2002) suggested the WD sample is largely complete. All three have colors redder than typical WDs, suggesting they may in fact be subdwarfs contaminating the WD region of the RPM diagram.

The faintness of the WDs selected via the $(B - R)$ RPM diagram suggests they are all quite distant, and indeed the distance estimates according to the relation of Oppenheimer et al. (2001) show the nearest to be at 40 pc.

TSN XXV discusses the 46 previous WD candidate discoveries, while the current effort adds 97 objects to this sample. In total we estimate 17 to be within 25 pc, of which 7 are from this paper. TSN XXV discusses parallax results from CTIOPI for four of these WDs, confirming they are within 25 pc. Spectroscopic observations are underway for unconfirmed WD discoveries.

5.4. New Cool Subdwarf Candidates

Table 5 provides the first five of the 557 cool subdwarf candidates. Because of their faintness compared to their similarly colored main-sequence counterparts, the distance estimates reported are too large and are listed in brackets in Tables 2 and 5. Figure 4 shows histograms of subdwarfs found in previous SCR searches as well as this work. The top plot shows we find more subdwarfs in the bin from $0\farcs18\ \mathrm{yr}^{-1} \leqslant \mu \leqslant 0\farcs20\ \mathrm{yr}^{-1}$, but fewer subdwarfs with $\mu > 0\farcs30\ \mathrm{yr}^{-1}$ than previous works. The bottom plot shows we discover redder subdwarfs in this work. The mean $(V - K)$ color[6] of subdwarfs discovered in previous efforts is 3.2, while it is 3.8 in this effort. The redness may be explained in part by these systems being more distant discoveries than those from previous papers, and hence being affected by interstellar reddening. In the previous searches, the reddest subdwarf candidate has $(V - K) \sim 5.21$ (SCR 0020-2642B), while here we find one with $(V - K) \sim 5.74$ (SCR 1522-0244), which is similar in color to LHS 377, an M7.0 subdwarf (Gizis (1997), $(V - K) = 5.76$). The H-R diagrams in Gizis (1997) and Jao et al. (2005) show that there are very few cool subdwarfs redder than M5.0. In recent years a few L type subdwarfs have been identified (Burgasser et al. 2009, and references therein), but more are needed to explore the hydrogen-burning limit that comprise the end of main sequence. This work has increased the number of cool subdwarf candidates, but future astrometric and spectroscopic observations are needed to confirm them.

5.5. Common Proper Motion Systems

We have found 24 potential CPM systems, including one triple, listed in Table 6. Of these, 19 consist entirely of new discoveries, while the other five have at least one known component. In Table 6 we provide distance estimates for all components, proper motions, separations, and position angles for both proper motions and separations.

Systems were found by one of two methods. First, during the blinking process systems were noted as having similar proper motion and position angles. Second, an automated search for companions within a radius of 1200″, as well as

[6] The V magnitudes are estimated using the mean of the B and R magnitudes.

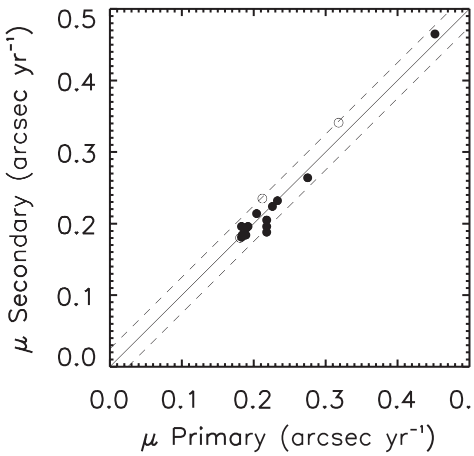

Figure 5. Plot of the proper motion of the primary vs. that of its companion in common proper motion systems. The solid line denotes perfect agreement between the two proper motions, while the dashed lines indicate limits of 0″.025 yr^{-1} in accordance with our uncertainties. Filled circles represent pairs in which both members had data from the automatic phase of the search. Open circles denote pairs in which proper motion data for at least one component were gathered manually.

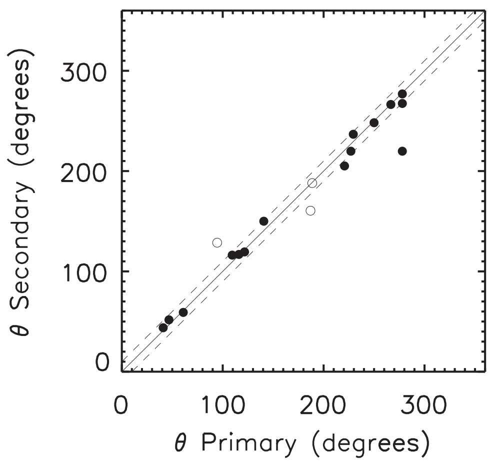

Figure 6. Plot of the position angle of the proper motion of the primary vs. that of its companion in common proper motion systems. The solid line denotes perfect agreement between the two proper motions, while the dashed lines indicate limits of 10° in accordance with our uncertainties. Filled circles represent pairs in which both members had data from the automatic phase of the search. Open circles denote pairs in which proper motion data for at least one component were gathered manually.

$\Delta\mu < 0''.025$ yr^{-1} and Δ P.A. $< 10°$, was performed around each object in the search.

The database from which the initial sample was drawn is a version of the database optimized for high proper motion objects. For systems noticed by eye that were not in the initial search sample, we manually gathered SuperCOSMOS data from the SSS Web site. For moving objects, the SSS online catalogs tend to be less reliable and less complete, even at relatively low proper motions, as discussed in TSN XXV. We divide the table into two sections, probable and possible systems. Probable systems have μ and P.A. within 0″.025 yr^{-1} and 10°, respectively, as well as consistent distance estimates, while probable systems appear to be comoving on plate images but either lack data to confirm CPM or have data that suggest otherwise.

Figures 5 and 6 compare the proper motion sizes and position angles for components of multiple systems, respectively. Systems marked with solid points are those with both components retrieved during the initial automated search, and tend to have better agreement between these values, particularly for the proper motions. Systems for which at least one component had its proper motion and position angle data gathered manually from the SSS database are marked with open circles.

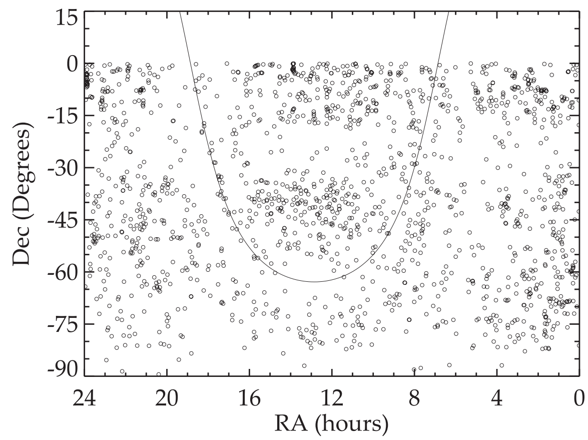

Figure 7. Sky distribution of newly discovered systems. The curve represents the Galactic plane.

5.6. Sky Distribution of SCR Systems

Figure 7 shows the sky distribution of systems presented in this paper, with the curve representing the Galactic plane. As in TSN XXV, we note a string of new systems superimposed on background dust in the Galactic plane. We also note a lack of discoveries in the areas near the Galactic center not obscured by dust. When compared to Figure 7 in TSN XXV, the NLTT system distribution in the southern sky, we note a similarly high density of new systems in areas searched less thoroughly by Giclas and Luyten. In the area between declinations −15° and −30°, there are relatively few new systems. This is because this region of the sky has been searched particularly deeply, notably by Giclas and Luyten as well as the LEHPM survey. A similar pattern exists, but was not noted, in the distribution presented in Figure 6 of TSN XXV.

5.7. Comments on Individual Systems

Here we highlight a few of the 1584 systems reported from this portion of the SCR search. These represent extremes in proximity, color (both blue and red), and/or sky separation.

SCR 0058-6905 is the second nearest WD candidate, estimated to be at 12.1 pc, and one of three within the 13 pc limit of completeness according to Holberg et al. (2002). Its nature as a WD is somewhat questionable, however, as its $(B - R)$ color is redder than most WDs.

SCR 0128-7401 is the third nearest WD candidate, estimated to be at 12.8 pc, and one of three within the 13 pc limit of completeness according to Holberg et al. (2002). Its optical and near IR colors, however, are redder than most WDs, calling in to question its nature.

SCR 0221-0143 is the bluest system discovered in this search with $(R - J) = 0.12$. It is a WD candidate at 46.5 pc.

SCR 0307-4654A/LEHPM 1-3098 is the most widely separated system in this search, with a separation of 1180″.3. Using the mean distance of the system, this gives a projected sky separation of nearly 200,000 AU. While this system may be a random alignment of two unrelated stars, if the two stars comprise a system, it would be among the most weakly bound and widest systems known.

SCR 1546-5534 is the nearest star revealed by this search. It is the second closest system revealed by the SCR searches, after SCR 1845-6357AB at 3.5 pc, as reported in Henry et al. (2006). With $(R - J) = 7.01$, it is also the reddest object revealed by the SCR searches. We note that this object only has eight plate relations, with distance estimates ranging from 3.1 to 15.7 pc, calling into question its estimate of 6.7 pc. Even so, it is worthy of follow up and is currently being observed as part of RECONS' ongoing parallax program at the CTIO 0.9 m telescope.

SCR 2045-1411 is the nearest estimated WD candidate at 10.7 pc, and one of three that lie within the 13 pc limit of completeness according to Holberg et al. (2002). It is, however, unlikely to be an actual WD. Its $(B - I)$ and $(J - K)$ colors are significantly redder than known WDs, and unlike such known WDs, it satisfies all 11 red dwarf plate relations. It is likely a cool subdwarf candidate contaminating the WD area of the RPM diagram.

6. DISCUSSION

This paper completes an SCR sweep of the southern sky to $R = 18.0$ for systems with $\mu \geqslant 0\farcs18$ yr^{-1}. In total, we have found 6308 new proper motion systems, of which 1584 are first reported in this paper, representing an increase of 33% over the previous count. A total of 155 red dwarfs estimated to be within 25 pc, including 10 within 10 pc, have been found, of which three and one originate from this paper, respectively. We have found an additional 97 WD candidates, bringing the total to 143, and an additional 557 cool subdwarf candidates, bringing the total to 1155.

This paper is unique for the sheer numbers of WD and subdwarf candidates revealed, with total counts that have tripled and doubled, respectively. Given the nature of their selection, there is obviously some contamination of the samples, but regardless, this represents a substantial increase. Of the 97 WDs presented here, seven are estimated to lie within 25 pc. The subdwarfs presented here are redder and cooler than those previously discovered, helping fill in a currently underrepresented sample of cool subdwarfs discovered by these searches.

As part of our Cerro Tololo Inter-American Observatory Parallax Investigation (CTIOPI), an astrometry program carried out at the CTIO 0.9 m (Jao et al. 2005; Henry et al. 2006; Subasavage et al. 2009; Riedel et al. 2010; Jao et al. 2011), we aim to obtain accurate trigonometric parallaxes for systems estimated to be near the Sun from the categories of 25 pc objects, WDs, and cool subdwarfs. While the sheer number of candidates for observation means we can only select the best gems, the SCR search efforts will provide a wealth of targets for particular attention in large-scale astrometric efforts such as *Gaia* and LSST. Such observations will help us map the solar neighborhood more accurately than ever before.

The RECONS effort is supported by the National Science Foundation through grant AST 09-08402. Funding for the SuperCOSMOS Sky Survey was provided by the UK Particle Physics and Astronomy Research Council. N.C.H. thanks colleagues in the Wide Field Astronomy Unit at Edinburgh for their work in making the SSS possible; particular thanks go to Mike Read, Sue Tritton, and Harvey MacGillivray. This research has made use of results from the SAO/NASA Astrophysics Data System Bibliographic Services, the SIMBAD and VizieR databases operated at CDS, Strasbourg, France, and the Two Micron All Sky Survey, which is a joint project of the University of Massachusetts and the Infrared Processing and Analysis Center, funded by NASA and NSF.

REFERENCES

Bakos, G. A., Sahu, K. C., & Nemeth, P. 2002, ApJS, 141, 187
Boyd, M. R., Winters, J. G., Henry, T. J., et al. 2011, AJ, 142, 10 (TSN XXV)
Burgasser, A. J., Lépine, S., Lodieu, N., et al. 2009, in AIP Conf. Ser. 1094, 15th Cambridge Workshop on Cool Stars, Stellar Systems, and the Sun, ed. E. Stempels (Melville, NY: AIP), 242
Deacon, N. R., Hambly, N. C., & Cooke, J. A. 2005, A&A, 435, 363
Deacon, N. R., & Hambly, N. C. 2007, A&A, 468, 163
Finch, C. T., Henry, T. J., Subasavage, J. P., Jao, W. C., & Hambly, N. C. 2007, AJ, 133, 2898 (TSN XVIII)
Finch, C. T., Zacharias, N., & Henry, T. J. 2010, AJ, 140, 844
Giclas, H. L., Burnham, R., & Thomas, N. G. 1971, Lowell Proper Motion Survey Northern Hemisphere. The G Numbered Stars. 8991 Stars Fainter than Magnitude 8 with Motions > $0\farcs26$/year (Flagstaff, AZ: Lowell Observatory)
Giclas, H. L., Burnham, R., & Thomas, N. G. 1978, Lowell Obs. Bull., 8, 89
Gizis, J. E. 1997, AJ, 113, 806
Hambly, N. C., Henry, T. J., Subasavage, J. P., Brown, M. A., & Jao, W. C. 2004, AJ, 128, 437 (TSN VIII)
Henry, T. J., Subasavage, J. P., Brown, M. A., et al. 2004, AJ, 128, 2460 (TSN X)
Henry, T. J., Jao, W. C., Subasavage, J. P., et al. 2006, AJ, 132, 2360 (TSN XVII)
Holberg, J. B., Oswalt, T. D., & Sion, E. M. 2002, ApJ, 571, 512
Jao, W.-C., Henry, T. J., Subasavage, J. P., et al. 2005, AJ, 129, 1954 (TSN XIII)
Jao, W.-C., Henry, T. J., Beaulieu, T. J., & Subasavage, J. P. 2005, AJ, 129, 1954
Jao, W.-C., Henry, T. J., Subasavage, J. P., et al. 2011, AJ, 141, 117 (TSN XXIV)
Lépine, S. 2005, AJ, 130, 1247
Lépine, S. 2008, AJ, 135, 2177
Luyten, W. J. 1979, LHS Catalogue (Minneapolis, MN: Univ. of Minnesota Press)
Luyten, W. J. 1980, NLTT Catalogue (Minneapolis, MN: Univ. of Minnesota Press)
Luyten, W. J. 1980, Proper Motion Survey with the 48-inch Telescope, Vol. 55 (Minneapolis, MN: Univ. of Minnesota Press), 1
Oppenheimer, B. R., Hambly, N. C., Digby, A. P., Hodgkin, S. T., & Saumon, D. 2001, Science, 292, 698
Pokorny, R. S., Jones, H. R. A., & Hambly, N. C. 2003, A&A, 397, 575
Riedel, A. R., Subasavage, J. P., Finch, C. T., et al. 2010, AJ, 140, 897 (TSN XXII)
Subasavage, J. P., Henry, T. J., Hambly, N. C., Brown, M. A., & Jao, W. C. 2005a, AJ, 129, 413 (TSN XII)
Subasavage, J. P., Henry, T. J., Hambly, N. C., et al. 2005b, AJ, 130, 1658 (TSN XV)
Subasavage, J. P., Jao, W. C., Henry, T. J., et al. 2009, AJ, 137, 4547 (TSN XXI)